

TimesNet-Gen: Deep Learning-based Site Specific Strong Motion Generation

Baris Yilmaz, Bevan Deniz Cilgin, Erdem Akagündüz, *Senior Member, IEEE*, and Salih Tileylioglu

Abstract—Effective earthquake risk reduction relies on accurate site-specific evaluations. This requires models that can represent the influence of local site conditions on ground motion characteristics. In this context, data driven approaches that learn site controlled signatures from recorded ground motions offer a promising direction. We address strong ground motion generation from time-domain accelerometer records and introduce the TimesNet-Gen, a time-domain conditional generator. The approach uses a station specific latent bottleneck. We evaluate generation by comparing HVSR curves and fundamental site-frequency f_0 distributions between real and generated records per station, and summarize station specificity with a score based on the f_0 distribution confusion matrices. TimesNet-Gen achieves strong station-wise alignment and compares favorably with a spectrogram-based conditional VAE baseline for site-specific strong motion synthesis. Our codes are available via a public repo.

Index Terms—strong ground motion, deep learning, conditioned generation, HVSR, fundamental site frequency, seismology

I. INTRODUCTION

Earthquakes have historically led to significant loss of life and extensive economic damage. The 2023 Turkey–Syria earthquakes had a death toll exceeding 53,000, caused more than \$103 billion in economic losses, and affected over 13 million people [1]. Although these impacts cannot be fully eliminated, combining source characterization, recurrence modeling, ground-motion prediction, site-specific hazard assessment, and resilient design practice has substantially reduced earthquake related damage. Among these components, site effects are especially critical because local geology can heavily modify ground shaking.

Strong motion recordings capture ground acceleration from seismic stations during earthquakes. While studies such as [2] and [3] have explored the use of deep learning for site-specific seismic signal analysis, it remains challenging to effectively capture the complex temporal and spectral patterns present in seismic recordings. As discussed in [4], there is still no foundational deep learning model that can effectively represent the complex temporal and spectral patterns of these recordings. Developing such a model is essential, as a system capable of generalizing and conditionally generating strong motion

Baris Yilmaz and Assoc. Prof. Erdem Akagündüz are with the Department of Modeling and Simulation, Graduate School of Informatics, Middle East Technical University, Ankara, Türkiye (e-mail: yilmaz.baris_01@metu.edu.tr; akaerdem@metu.edu.tr).

Bevan Deniz Cilgin is with the Department of Data Informatics, Graduate School of Informatics, Middle East Technical University, Ankara, Türkiye (e-mail: cilgin.bevan@metu.edu.tr).

Assist. Prof. Salih Tileylioglu is with the Department of Civil Engineering, Kadir Has University, Istanbul, Türkiye (e-mail: salih.tileylioglu@khas.edu.tr).

signals would significantly enhance future seismic hazard assessment and mitigation methods. In addition, with such a foundational model, it would become possible to enhance other downstream seismic tasks such as P- and S-wave detection for early warning systems and parameter estimation in earthquake engineering applications.

In this paper, we hypothesize that strong motion waveforms can be effectively conditioned in a deep generative framework using station specific (or more generally site specific) identifiers, and their validity and station relevance can be evaluated through the analyses of site’s fundamental frequency. While existing data driven studies utilize conditioning for the generation of strong motion data on physical parameters such as magnitude, distance, and velocity using deep generative models [5], to the best of our knowledge, there are no studies that have explored conditioning solely based on station-specific identifiers such as station IDs. Station conditioning enables the model to isolate and learn site-specific patterns that are characteristically consistent but naturally variable across events. This poses a significant challenge, as most sites have only a limited number of available records, and traditional conditioning methods often fail to capture the underlying site-dependent patterns reliably. Thus, the reliability of these site-specific simulations can be limited.

We introduce TimesNet-Gen, a time-domain conditional model built by adapting TimesNet [6]. TimesNet has demonstrated strong performance on complex, multi-periodic time signals by extracting multi-scale temporal patterns. We note that seismic strong-motion waveforms exhibit similar periodic structure. While TimesNet has primarily been applied to short-term forecasting, imputation, classification, and anomaly detection, we first extend the architecture to configure it as an autoencoding model that optimizes a time-domain mean squared error (MSE) objective for reconstruction and observe competitive performance. We then convert this reconstruction model into a generative architecture by reusing the same decoder and inserting a latent bottleneck together with station-ID conditioning.

As a baseline, we train a convolutional VAE [7] on amplitude/phase spectrograms with station-ID conditioning. In order to benchmark both approaches, site-frequency based analyses are carried out. We employ strong-motion recordings from the Disaster and Emergency Management Presidency of Türkiye (AFAD) database [8] and adopt a two-phase straining strategy: unconditioned and unsupervised pretraining on the full corpus, followed by fine-tuning on five stations (348 records) for station-conditioned generation.

Our contributions are as follows. (i) We propose the TimesNet-Gen, a novel time-domain, station-conditioned deep

learning architecture. (ii) In addition to a classical site-frequency-based strong motion analysis method, an evaluation metric that uses fundamental site-frequency distributions calculated from generated records for a given station (site) is proposed and used for evaluation. (iii) Unlike previous seismological predictors [9] [10] [11] [12], our approach learns directly from data without extensive parameter tuning, ground-motion equations, or strong theoretical assumptions.

A. Related Work

The related literature on classical and deep learning based seismic data generation and evaluation is summarized below. 1) *Classical Methods on Seismic Data Synthesis*: can be broadly categorized into three types: empirical [9] [10], semi-empirical [11], and physics-based [12]. In general, classical methods involve simplifying assumptions and computational cost for broadband simulations. These approaches often struggle to reproduce the fine-scale variability and nonstationary temporal-spectral behavior of strong-motion recordings, and methods that model such nonstationarity more realistically generally require high computational cost, while faster empirical and semi-empirical approaches capture only limited aspects of it. The drawbacks of the mentioned methods make generative models advantageous for transforming the complex nature of seismic waves into valuable insights, as they learn directly from the data and have a low computational cost. For a general overview of classical and other approaches, the reader may refer to [13].

2) *Deep Learning-based Seismic Data Generation*: models are deep learning-based frameworks for creating synthetic seismic data and learn directly from existing data distributions. Variational AutoEncoders (VAEs) have been widely used for this task due to the fact that they can be trained with smaller sets and create a latent space that can be used to easily sample new data [14] [15]. Another deep generative architecture, generative adversarial networks (GANs) can create high-fidelity samples; however, their training is challenging due to instability during training and mode collapse problems [16] [17] [18]. Diffusion models generate data from random noise by iteratively learning the reverse of a noise perturbation process. However, they require high computational power due to the numerous refinement steps involved [19] [20].

3) *Evaluation*: Evaluating the output of generative models is a complex task. The primary objective of a deep generative model is typically to implicitly or explicitly model the training set distribution. However, assessing individual signals in terms of realism, diversity, or other qualities requires careful analysis. While off-the-shelf methods exist for vision-based generation, such as Fréchet Inception Distance (FID) [21], or text-based generation, including BLEU and ROUGE scores [22], there are no established standards for evaluating generated seismic data due to the limited number of studies in this domain.

Regarding the evaluation of simulated seismic data [23], prior works commonly assess intensity measures, frequency-domain similarity, or performance improvements in downstream tasks. Common methods for evaluating generated seismic samples include comparing the intensity measures (IMs)

of generated records with those of real records [18] [19], assessing metrics in the frequency domain and waveform shape [24] [20], and measuring the impact of generated samples on the performance of main tasks, such as waveform classification [16].

However, approaches to evaluate simulated data are not fully sufficient for assessing the representative quality of a distribution of generated sets, which is the main goal in generative processes. In this work, we validate our generated samples using site-frequency distributions associated with the waveforms, which is, to the best of our knowledge, novel in the literature. Details of this evaluation approach are provided in the following sections.

II. METHODOLOGY

We benchmark two approaches for strong-motion reconstruction and conditional generation: the proposed TimesNet-Gen and conditional VAE baseline. Below, the details of the architectures, station-id conditioning, generative sampling methods, input data preprocessing steps, training strategies, and utilized evaluation metrics are presented.

A. TimesNet-Gen

The original TimesNet model [6] introduces temporal 2D-variation modeling for general time series, where the 1D sequence is decomposed into multiple period-aligned 2D slices by selecting top- k dominant periods from the frequency domain. For each selected period p , the sequence is reshaped into a $(T/p, p)$ grid so that intraperiod-variation (within a period) appears along columns and interperiod-variation (across periods at the same phase) appears along rows. Each grid is processed by a parameter-efficient, Inception-style 2D convolutional branch that captures temporal patterns across short and long contexts. Branch outputs are aggregated with soft, period-dependent weights and merged through a residual path; a lightweight linear layer then projects features back to the original number of signal components (e.g., three acceleration channels). When clear periodicity is absent, variations are dominated by intra-period structure, which the backbone handles as the limiting case of very long periods. Prior work used this backbone for forecasting, imputation, classification, and anomaly detection.

Building on this backbone, we develop a time-domain conditional generative model, namely “TimesNet-Gen”, for reconstruction and station-specific conditional generation. The adaptation preserves the original encoder, includes an additional decoder, introduces a latent bottleneck, and realizes station-ID conditioning via channel-wise feature modulation inside the so-called “timesblocks” (Figure 1).

The backbone follows the standard TimesNet temporal block design, applying FFT-based period selection and multi-kernel 2D convolutions. We operate directly on multi-channel acceleration records $x \in \mathbb{R}^{T \times C}$ (N-S, E-W, V) at $F_s=100$ Hz. Sequences are center-aligned: if longer than the target length, a center crop around the midpoint is taken; if shorter, symmetric zero-padding is applied around the midpoint to reach

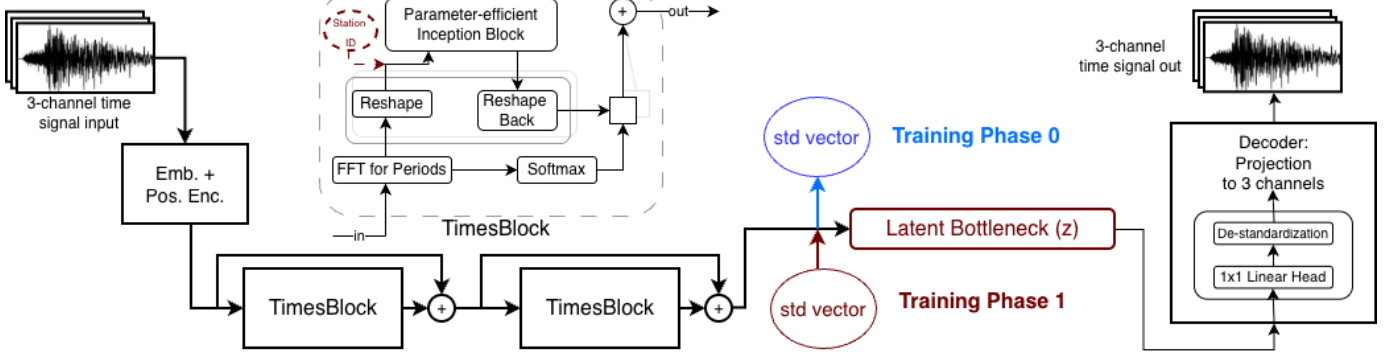


Fig. 1: TimesNet-Gen architecture.

($\text{seq_len} + \text{pred_len}$). We apply per-sequence, per-channel standardization and de-normalize outputs before computing time-domain losses to preserve the original scale.

1) *Conditioning*: To be able to generate station (or site)-specific records, we inject station conditioning into the times-blocks models. By providing one-hot encoded station IDs ($s \in \{0, \dots, S-1\}$), a conditioning channel is concatenated to the 2D feature maps before the convolutions and projected back to d channels via a 1×1 convolution.

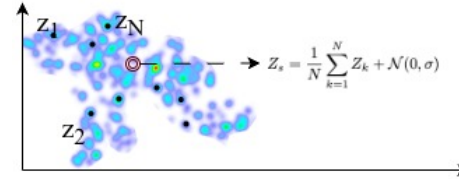
We introduce a latent bottleneck between the encoder and decoder parts. The latent code is produced by the encoder and propagated to the decoder without variational sampling or a KL prior, as in classical VAEs. Because TimesNet-Gen does not include a regularization loss that shapes the latent space into a Gaussian-like prior distribution; an alternative sampling procedure is applied, as explained in the following subsection.

2) *Sampling*: Because the proposed bottleneck latent space is not forced to have a prior distribution shape (for the sake of better reconstruction), we follow a straightforward bootstrap aggregating technique. Figure 2 illustrates the k -sample latent space vector averaging pipeline, and Eq. (2) formalizes sampling process. To introduce controlled diversity while preserving station characteristics, we average N (selected as 5 in our experiments) encoder features (i.e. latent codes) from the a specific station record pool and decode the mixed representation under the target station label. We also add gaussian noise of unit standard deviation σ , where σ is calculated from all latent codes of a specific station's records.

$$Z_s = \frac{1}{N} \sum_{k=1}^N Z_k + \mathcal{N}(0, \sigma) \quad (1)$$

B. Variational Autoencoders

Variational Autoencoders (VAEs) [25] are generative models that learn a probabilistic mapping between observed data and a lower-dimensional latent space. They consist of an encoder and a decoder that compress and reconstruct the data, enabling the generation of new samples. The proposed variational autoencoder consists of a convolutional encoder and a symmetric deconvolutional decoder. The encoder employs

Fig. 2: TimesNet-Gen sampling via k -sample encoder-feature averaging within a station pool.

four consecutive convolutional layers with 3×3 kernels and Leaky ReLU activations, followed by a flattening operation and two linear layers that produce the latent mean and standard deviation parameters. Latent variables are sampled using the reparameterization trick and passed to the decoder, which begins with a linear transformation and reshaping step. The decoder comprises four transposed convolutional layers with 3×3 kernels and Leaky ReLU activations, concluding with a sigmoid output layer that reconstructs the input.

1) *Latent Space Conditioning*: To incorporate station information into the generative process, similarly to the TimesNet-Gen, the VAE is conditioned in the second training phase. The conditioning is done only in the second training phase and for the VAE, this second training phase, includes two separate conditioning sub-phases. In the first sub-phase, the model is conditioned using one-hot encoded class priors. Each class is assigned a distinct prior mean vector μ_p constructed by tiling one-hot encodings across the latent dimensions, while the prior variance is fixed to $\sigma_p^2 = 1$. To ensure separable priors, the latent dimension is chosen as a multiple of the number of classes (five in this case), resulting in a 510-dimensional latent space. The Kullback–Leibler divergence term used in the loss is computed as

$$\begin{aligned} \text{KL}(q(z | c) \| p(z | c)) &= \dots \\ &+ \frac{1}{2} \sum \left(\frac{\sigma_q^2}{\sigma_p^2} + \frac{(\mu_q - \mu_p)^2}{\sigma_p^2} - 1 - \log \frac{\sigma_q^2}{\sigma_p^2} \right) \end{aligned} \quad (2)$$

where μ_q and σ_q^2 denote the encoder-predicted mean and variance, respectively, and (μ_p, σ_p^2) correspond to the parameters

of the class-specific prior distribution. Here, $p(z | c)$ represents the class-conditioned prior.

In the second phase, the latent space is further refined to sharpen the class clusters, following the approach of Mousavi et al. [26]. Encoded representations z_i are obtained from the first phase, and initial cluster centers μ_j are computed as the mean of samples belonging to each class. Cluster membership probabilities are estimated as

$$q_{ij} = \frac{(1 + \|z_i - \mu_j\|^2)^{-1}}{\sum_j (1 + \|z_i - \mu_j\|^2)^{-1}}, \quad (3)$$

and a sharpened target distribution is defined as

$$p_{ij} = \frac{q_{ij}^2}{\sum_i q_{ij}}. \quad (4)$$

The clustering loss \mathcal{L}_c is given by the Kullback–Leibler divergence between the sharpened and soft assignment distributions, and is added to the original VAE objective with a weighting factor a (100 in our experiments), yielding the final loss function

$$\mathcal{L}_{\text{final}} = \mathcal{L}_{\text{VAE}} + a \mathcal{L}_c. \quad (5)$$

2) Input Preprocessing: The aim of these preprocessing steps is to ensure that both amplitude and phase information can be effectively learned by the model while preserving the essential structural characteristics of the signal. In the preprocessing pipeline, spectrograms containing both amplitude and phase information were generated for each seismic record. First, short-time Fourier transform (STFT) is applied to all three channels of each record to produce amplitude and phase spectrograms, resulting in a multi-channel representation for each recording. The amplitude spectrograms are then converted to a logarithmic decibel (dB) scale to make them more perceptually meaningful and to facilitate the learning process. Phase spectrograms, initially obtained as wrapped phases within the range of $-\pi$ to π due to the FFT, exhibited discontinuities along the time axis; these are corrected using phase unwrapping to produce a continuous and smooth phase profile.

In order to be able to evaluate the results and compare them to TimesNetGet outputs, the spectrograms are converted back to time-domain signals. This was achieved by first denormalizing the amplitude and phase spectrograms, transforming the amplitude spectrograms from the logarithmic scale back to linear values, and then combining the amplitude and phase components before applying the inverse short-time Fourier transform.

C. Dataset

In our experiments, we employ strong-motion recordings from the Disaster and Emergency Management Presidency of Türkiye (AFAD) database [8] (36,417 records, 2012–2018). As explained in the following subsection we utilize two separate sets in order to adopt a two-phase training schedule. The first phase of training utilizes an unsupervised pretraining scheme on the entire corpus, followed by the second phase,

TABLE I: Properties of the Selected Stations

Station Id	Location	f_0	no. of rec.
2020	Tavas / Denizli	5.1 Hz	71
4628	Afsin / Kahramanmaraş	1.8 Hz	38
0205	Kahta / Adiyaman	2.6 Hz	98
1716	Ayvacık / Çanakkale	6.4 Hz	110
3130	Defne / Hatay	12.8 Hz	31

where the models are fine-tuned on records collected from five stations (a total of 348 records that were not included in the first phase) for station-conditioned generation. While selecting these stations, our criterion was finding stations with different site properties to test the generative model's ability to generate distinct classes. Hence, we chose five stations with different fundamental site frequencies. Some of the fundamental frequencies reported here (specifically for stations 2020 and 0205) differ from what is reported in AFAD website due to differences in the calculation method. Fundamental site frequency is typically calculated empirically from the horizontal-to-vertical spectral ratio (HVS) analysis of ambient recordings [27] as well as earthquake recordings [28] [29]. In this study we compute based on using strong motions signals, [28] [29]. The five stations used in this study and their identified fundamental frequencies are given in Table I.

D. Two-Phase Training

Both models are trained with a two-phase strategy. Models are first trained in an unsupervised manner with no conditioning, so as to construct a base latent code space. In the second phase, we fine-tune the model with station conditioning while injecting controlled Gaussian noise based on the stored standard deviations.

For both models the conditioning information is not introduced in the first training phase. Phase 0 is primarily used to learn the latent representation and to obtain statistical properties of the encoder features. In the second phase, station-specific conditioning is applied according to each method's strategy. For cross-validation purposes, the 348 records from the selected stations used in fine-tuning are excluded from the first-phase training.

To assess whether TimesNet-Gen's station-specific performance stems from explicit station conditioning (via station ID embeddings) or from its sampling strategy (selecting samples from the same station), an additional experiment was conducted. A single-phase, fully unsupervised TimesNet-Gen model was trained without any station conditioning, and generation for the five target stations was performed in a zero-shot manner by feeding only their waveforms to the encoder. The results remained consistent with the two-phase conditioned approach. This indicate that the model's ability to capture station characteristics is not derived from explicit station ID embedding, but rather from the learned latent representations based on waveform features alone. The latent representations naturally encode site-specific response properties in an unsupervised manner, and the station-specific sampling strategy effectively leverages this implicit clustering. Results are discussed and presented in the following section.

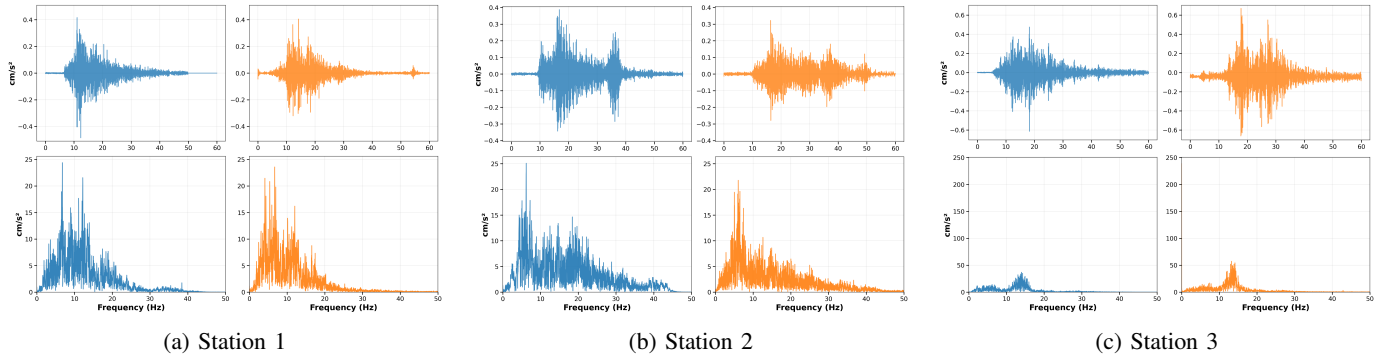


Fig. 3: Left: Real samples from the dataset. Right: similar TimesNet-Gen generated. Bottom: Corresponding Fourier amplitude spectra. Results are shown for three different stations.

E. Evaluation

To analyze the generation quality, two methods: a spectral and the proposed distribution-based metric are used.

1) *Spectral Analysis*: The characteristics of earthquake recordings depend on several factors, including source, path, and site effects [30]. One key site effect is the modification and amplification of ground motions through resonance, which occurs when incoming seismic waves contain energy close to the site frequency. The fundamental site frequency (f_0) is a critical parameter that represents site response and depends on the thickness and properties of the underlying soil layer. As stated earlier we use strong motion signals recorded at the sites to calculate (f_0). The calculation procedure is summarized below.

Horizontal-to-vertical spectral ratio (HVSR) curves are calculated using signals recorded from three channels: north-south ($H_1(t)$), east-west ($H_2(t)$), and vertical ($V(t)$) at the stations. First, amplitude spectra are calculated, $|H_1(f)|$, $|H_2(f)|$, and $|V(f)|$, then average horizontal amplitude is found using Eq. 6:

$$|H(f)| = \sqrt{\frac{|H_1(f)|^2 + |H_2(f)|^2}{2}} \quad (6)$$

Finally, the HVSR curve is constructed by dividing the average horizontal amplitude by the vertical amplitude spectra for each frequency.

In the HVSR curve, the lowest clear resonance peak is taken as the fundamental site frequency f_0 . Given that seismic waves are significantly amplified at or near the fundamental site frequency, it is critical to design structures with natural frequencies that avoid resonance with the site's predominant frequency. We restrict our analysis to the 1–20 Hz band and apply the same preprocessing and smoothing across all sources to ensure consistency.

2) *f_0 Distribution Confusion Matrices*: To further evaluate the physical consistency of the generated signals, we analyze the distributions of the calculated f_0 values obtained from both real and model-generated samples, for each station separately. For every N real sample of a station, we first compute the f_0 distribution. Then, using for both models, we generate and reconstruct same number of synthetic samples per station

and extract their corresponding f_0 values to build comparable distributions.

To quantify the similarity between these distributions, we employ the Jensen–Shannon Divergence (JSD). Since JSD measures dissimilarity, we convert it into a similarity score by taking its complement (i.e. 1 indicates perfect similarity, whereas 0 indicate no similarity). Next, we compute the intercorrelations for each station separately and filled them into a matrix. In this matrix, we expect the signals from the same station (real vs. TimesNet-generated vs. VAE-generated) to yield high similarity scores, while signals from different stations should produce low similarity scores, for each real vs. TimesNet-generated vs. VAE. The resulting 15x15 matrix corresponds to 5 stations (2020, 0205, 4628, 1716, 3130) \times 3 signal types (real, generated, reconstructed) and is specific to each model.

To evaluate the overall quality of each method, we calculated the distance between our matrices and an ideal matrix (each diagonal block corresponds to a station (3x3) with all entries set to 1, and all inter-station elements are 0) using Normalized Cross-Correlation (NCC). Related figures can be found in the Results section.

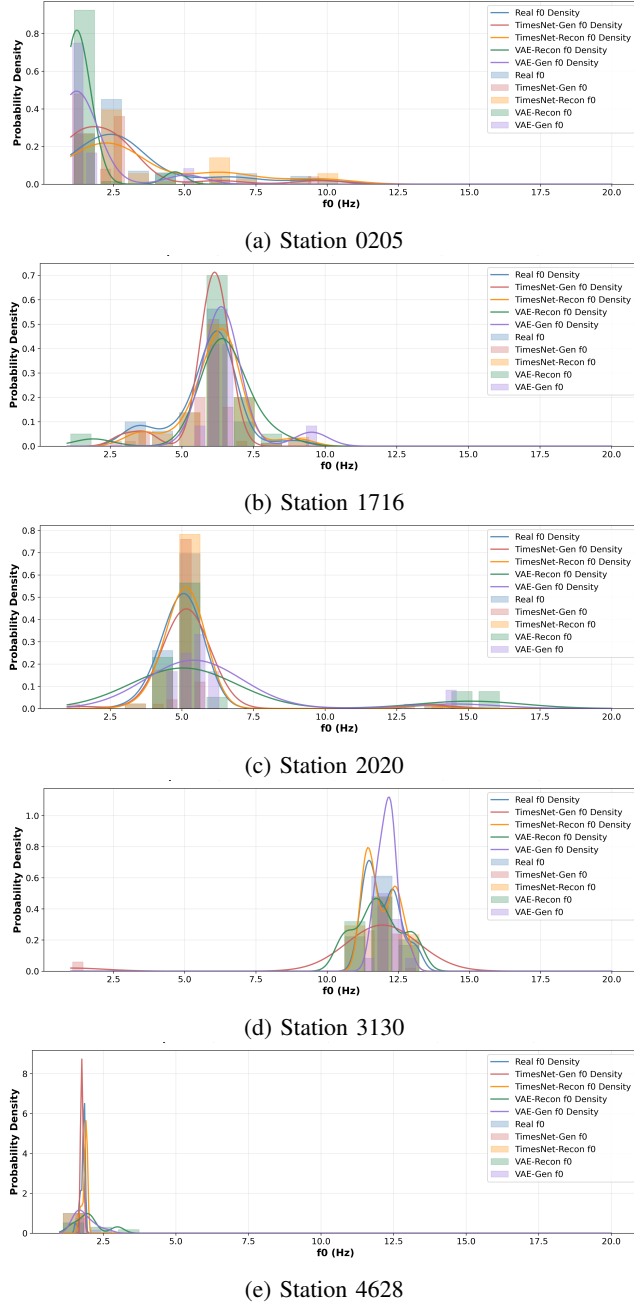
III. EXPERIMENTS AND RESULTS

A. Sample Results

We begin by visually analyzing some generated signals for each model. As seen in Figure 3, real and TimesNet-Gen generated sample E-W components exhibit earthquakes with varying durations and amplitudes, demonstrating that our sampling method successfully introduces variation by creating a continuous latent space. The bottom figures are the corresponding Fourier amplitude spectra, showing frequency behaviour similar to real samples. In the following, we focus on general spectral and frequency-domain evaluations, and assess how well each model captures station-dependent frequency content, dominant site frequencies, and overall HVSR behavior.

B. Spectral Analysis

For spectral analysis, we first present the f_0 distributions for real data, each model's reconstructed samples, and generated

Fig. 4: f_0 distributions for selected stations.

samples in Figure 4. We generate 50 samples to create a distribution and present these distributions. We also evaluate “reconstructed” results, which we obtain by feeding real signals through the encoder–decoder pathway and measuring reconstruction fidelity. In practice, this provides an upper bound on the generative quality we could expect from any sampling strategy. As seen in the figure, TimesNet performs better, with reconstruction quality remaining largely consistent across stations, whereas it degrades considerably for the VAE. TimesNet generates samples that follow the real f_0 distributions more closely, including at stations where the empirical distribution shows irregular or wide-spread behavior. In addition, its performance remains stable across different

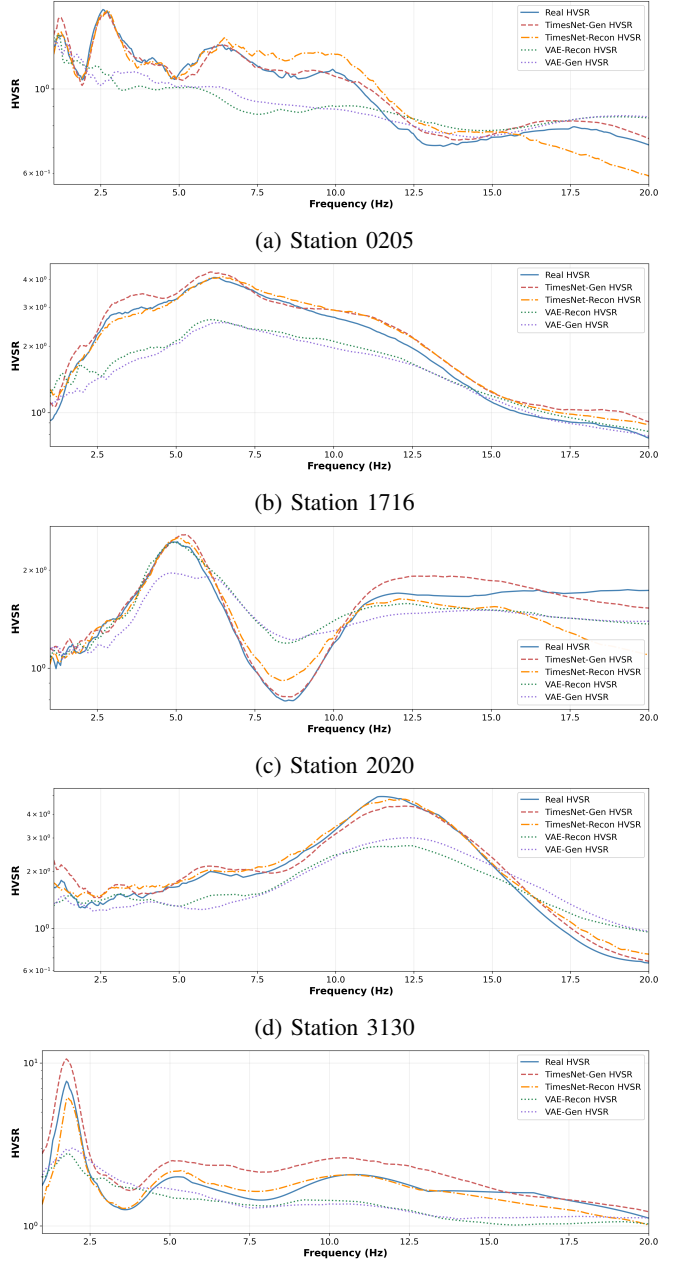


Fig. 5: Average HVSR curves for selected stations.

frequency ranges, indicating that the model captures station-specific spectral patterns more reliably.

Then, we analyse the *average* HVSR (average of all individual HVSR curves for a given category) plots separately for real data, each model’s reconstructed samples, and generated samples, in Figure 5. Results show that TimeNet-Gen demonstrates strong performance, even in stations 0205 and 4628, where it is able to capture the peak behavior of each individual HVSR curve. In contrast, VAE tends to deviate either above or below the actual peaks in most cases, and notably at station 0205, it fails to reproduce the sharp peak characteristics. These average distributions provide insight into the models’ ability to preserve site-specific frequency content.

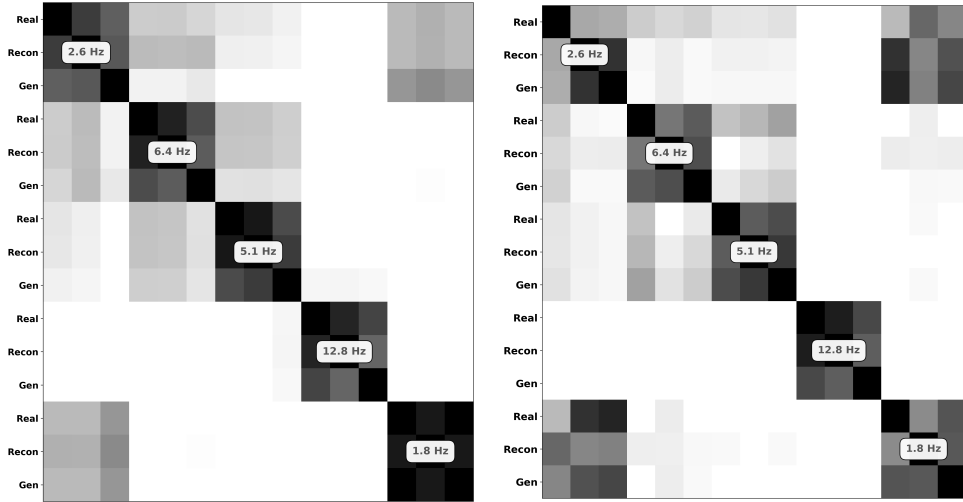


Fig. 6: f_0 distribution Confusion Matrices. Left: TimesNet-Gen (alignment score: 0.93), Right: VAE (alignment score: 0.81).

When different HVSR curves show consistent peak frequency and amplitude, they capture stable resonance characteristics of the site, emphasizing the need to represent these peaks accurately.

C. f_0 Distribution Confusion Matrices

Finally, we calculate the f_0 Distribution Confusion Matrices for each model, to evaluate the interstation discrimination and real vs model similarity. For each model separately in Figure 6, two 15×15 confusion matrices are provided. As seen from the figure, some stations (most notably 0205 and 4628) have close f_0 values, as also shown in Table I and Figure 6. A similar pattern is observed for stations 1716 and 2020, which also share comparable f_0 characteristics. Although close f_0 values reflect comparable dominant resonance frequencies, they do not fully describe overall site response, which can still differ across stations. Importantly, TimesNet-Gen distinguishes these stations despite their f_0 proximity, suggesting that the model captures additional waveform characteristics beyond the fundamental resonance alone. In contrast, the VAE baseline shows more ambiguity in these station pairs, with noticeably weaker separation and a tendency to mix stations that share similar f_0 values.

IV. CONCLUSIONS

In this work, we introduce TimesNet-Gen, a station-conditioned, time-domain deep learning model designed to generate realistic site-specific strong motion records. Our approach directly learns from seismic recordings, without relying on traditional ground-motion equations. We evaluate the model using f_0 distribution confusion matrices and median HVSR curves, demonstrating that TimesNet-Gen can reproduce both spectral and temporal characteristics observed in real recordings. Across multiple stations, the model captures key site-specific features, generating diverse yet physically plausible waveforms that align closely with real data. Station-wise comparisons further support this observation. Median HVSR curves and f_0 distributions for TimesNet-Gen closely match

real data across all five stations, showing tighter clustering and more consistent amplification patterns compared to VAE. HVSR curves, computed as the ratio of horizontal-to-vertical spectral amplitudes, exhibit similar character. Importantly, the VAE baseline we used was not a randomly selected or an arbitrary model; we explored multiple approaches to shape its latent space and reported the best-performing results as our baseline.

When conditioned on the same station, TimesNet-Gen generates waveforms with varying P and S-wave arrival times, amplitudes, and durations. Such variability is consistent with what occurs at a given site due to differences in earthquake sources and propagation paths, and the model reproduces this diversity without converging to a single waveform pattern. To further enhance the quality of the generated waveforms, future work will include the distributions of P and S wave arrival times, peak ground acceleration, duration, and other intensity related parameters into the evaluation process. TimesNet-Gen demonstrates strong potential for additional research directions: the model can be extended toward physics-guided or simulation-oriented earthquake generation, and its encoder's generalizable representations provide a foundation for downstream seismic tasks such as phase picking, ground-motion parameter estimation, or event classification.

V. ACKNOWLEDGEMENTS

This study was supported by the Middle East Technical University (METU) Scientific Research Projects (BAP) under grant number ADEP-704-2024-11482.

REFERENCES

- [1] U. N. D. Programme, “Two years on: A look at undp’s earthquake recovery efforts in turkey,” <https://www.undp.org/turkiye/news/two-years-look-undps-earthquake-recovery-efforts-turkiye>, 2025, accessed: 2025-09-20.
- [2] S. M. Mousavi and G. C. Beroza, “Bayesian-deep-learning estimation of earthquake location from single-station observations,” *IEEE Transactions on Geoscience and Remote Sensing*, vol. 58, no. 11, p. 8211–8224, Nov. 2020. [Online]. Available: <http://dx.doi.org/10.1109/TGRS.2020.2988770>

[3] B. Yilmaz, M. Türkmen, S. Meral, E. Akagündüz, and S. Tileylioglu, “Deep learning-based average shear wave velocity prediction using accelerometer records,” 2024. [Online]. Available: <https://arxiv.org/abs/2408.14962>

[4] Ümit Mert Çağlar, B. Yilmaz, M. Türkmen, E. Akagündüz, and S. Tileylioglu, “Exploring challenges in deep learning of single-station ground motion records,” 2025. [Online]. Available: <https://arxiv.org/abs/2403.07569>

[5] M. A. Florez, M. Caporale, P. Buabthong, Z. E. Ross, D. Asimaki, and M.-A. Meier, “Data-driven accelerogram synthesis using deep generative models,” 2020. [Online]. Available: <https://arxiv.org/abs/2011.09038>

[6] H. Wu, T. Hu, Y. Liu, H. Zhou, J. Wang, and M. Long, “Timesnet: Temporal 2d-variation modeling for general time series analysis,” 2023. [Online]. Available: <https://arxiv.org/abs/2210.02186>

[7] D. P. Kingma and M. Welling, “An introduction to variational autoencoders,” *Foundations and Trends in Machine Learning*, 2019. [Online]. Available: <https://www.nowpublishers.com/article/Details/MAL-056>

[8] M. Türkmen, S. Meral, B. Yilmaz, M. Cikis, E. Akagündüz, and S. Tileylioglu, “Deep learning-based epicenter localization using single-station strong motion records,” 2024. [Online]. Available: <https://arxiv.org/abs/2405.18451>

[9] N. A. Abrahamson and R. R. Youngs, “A stable algorithm for regression analyses using the random effects model,” *Bulletin of the Seismological Society of America*, vol. 82, no. 1, pp. 505–510, 1992.

[10] W. B. Joyner and D. M. Boore, “Peak horizontal acceleration and velocity from strong-motion records including records from the 1979 imperial valley, california, earthquake,” *Bulletin of the seismological Society of America*, vol. 71, no. 6, pp. 2011–2038, 1981.

[11] S. Arora, A. Joshi, P. Kumari, P. Kumar, S. K. Sah, S. Lal, and N. P. Singh, “Strong ground motion simulation techniques—a review in world context,” *Arabian Journal of Geosciences*, vol. 13, no. 14, p. 673, 2020.

[12] P. M. Mai, W. Imperatori, and K. B. Olsen, “Hybrid broadband ground-motion simulations: Combining long-period deterministic synthetics with high-frequency multiple s-to-s backscattering,” *Bulletin of the Seismological Society of America*, vol. 100, no. 5A, pp. 2124–2142, 2010.

[13] S. Rezaeian, J. P. Stewart, N. Luco, and C. A. Goulet, “Findings from a decade of ground motion simulation validation research and a path forward,” *Earthquake Spectra*, vol. 40, no. 1, pp. 346–378, 2024. [Online]. Available: <https://doi.org/10.1177/87552930231212475>

[14] K. Li, S. Chen, and G. Hu, “Seismic labeled data expansion using variational autoencoders,” *Artificial Intelligence in Geosciences*, vol. 1, pp. 24–30, 2020.

[15] P. Ren, R. Nakata, M. Lacour, I. Naiman, N. Nakata, J. Song, Z. Bi, O. A. Malik, D. Morozov, O. Azencot, N. B. Erichson, and M. W. Mahoney, “Learning physics for unveiling hidden earthquake ground motions via conditional generative modeling,” 2024. [Online]. Available: <https://arxiv.org/abs/2407.15089>

[16] Y. Li, B. Ku, S. Zhang, J.-K. Ahn, and H. Ko, “Seismic data augmentation based on conditional generative adversarial networks,” *Sensors*, vol. 20, no. 23, p. 6850, 2020.

[17] Y. Shi, G. Lavrentiadis, D. Asimaki, Z. E. Ross, and K. Azizzadenesheli, “Broadband ground-motion synthesis via generative adversarial neural operators: Development and validation,” *Bulletin of the Seismological Society of America*, vol. 114, no. 4, pp. 2151–2171, 2024.

[18] J. Yamaguchi, Y. Tomozawa, and T. Saka, “Site-specific ground-motion waveform generation using a conditional generative adversarial network and generalized inversion technique,” *Bulletin of the Seismological Society of America*, vol. 114, no. 4, pp. 2118–2137, 2024.

[19] A. Bergmeister, K. H. Palgunadi, A. Bosisio, L. Ermert, M. Koroni, N. Perraudin, S. Dirmeier, and M.-A. Meier, “High resolution seismic waveform generation using denoising diffusion,” 2024. [Online]. Available: <https://arxiv.org/abs/2410.19343>

[20] J. Jung, J. Lee, C. Jung, H. Kim, B. Jung, and D. Lee, “Broadband ground motion synthesis by diffusion model with minimal condition,” 2025. [Online]. Available: <https://arxiv.org/abs/2412.17333>

[21] M. Heusel, H. Ramsauer, T. Unterthiner, B. Nessler, and S. Hochreiter, “Gans trained by a two time-scale update rule converge to a local nash equilibrium,” in *NIPS*, 2017, pp. 6626–6637.

[22] C. Lin, “Rouge: A package for automatic evaluation of summaries,” in *Proc. ACL Workshop on Text Summarization Branches Out*, 2004, p. 10.

[23] C.-T. Chen, S.-C. Chang, and K.-L. Wen, “Stochastic ground motion simulation of the 2016 meinong, taiwan earthquake,” *Earth, Planets and Space*, vol. 69, no. 1, p. 62, 2017.

[24] Y. Matsumoto, T. Yaoyama, S. Lee, T. Hida, and T. Itoi, “Generative adversarial networks-based ground-motion model for crustal earthquakes in japan considering detailed site conditions,” *Bulletin of the Seismological Society of America*, vol. 114, no. 6, pp. 2886–2911, 2024.

[25] D. P. Kingma and M. Welling, “Auto-encoding variational bayes,” 2013. [Online]. Available: <https://arxiv.org/abs/1312.6114>

[26] S. M. Mousavi, W. Zhu, W. Ellsworth, and G. Beroza, “Unsupervised clustering of seismic signals using deep convolutional autoencoders,” *IEEE Geoscience and Remote Sensing Letters*, vol. 16, no. 11, pp. 1693–1697, 2019.

[27] Y. Nakamura, “A method for dynamic characteristics estimation of subsurface using microtremor on the ground surface,” *Railway Technical Research Institute, Quarterly Reports*, vol. 30, no. 1, 1989.

[28] J. Lermo and F. J. Chávez-García, “Site effect evaluation using spectral ratios with only one station,” *Bulletin of the seismological society of America*, vol. 83, no. 5, pp. 1574–1594, 1993.

[29] M. Yazdi, R. Motamed, and J. G. Anderson, “A new set of automated methodologies for estimating site fundamental frequency and its uncertainty using horizontal-to-vertical spectral ratio curves,” *Seismological Society of America*, vol. 93, no. 3, pp. 1721–1736, 2022.

[30] S. L. Kramer and J. P. Stewart, *Geotechnical earthquake engineering*. CRC Press, 2024.



Barış Yılmaz received the B.S. and M.S. degrees in Electrical and Electronics Engineering from Çankaya University, Ankara, Turkey, in 2019 and 2022, respectively. From 2020 to 2022, he worked as a Research Assistant in the Department of Electrical and Electronics Engineering at Çankaya University. He is currently a Ph.D. candidate with the Department of Modeling and Simulation, Middle East Technical University (METU), and a full-time doctoral researcher at METU AIRLab. His research interests include strong motion analysis and generative AI.



Bevan Deniz Çilgin received his B.S. degree in Electrical and Electronics Engineering from Middle East Technical University (METU), Ankara, Turkey, in 2021, and his M.S. degree from the METU Informatics Institute in 2025. His research interests include computer vision, deep learning, and signal processing.



Dr. Akagündüz holds several international patents and publications in these areas.



Salih Tileylioglu received his B.Sc. (1999) and M.Sc. (2002) degrees in Civil Engineering from Eastern Mediterranean University and Middle East Technical University, respectively. He earned his Ph.D. from the University of California, Los Angeles (UCLA) in 2008. After working in geotechnical engineering firms and obtaining a professional engineering license in the State of California, he served as an assistant professor at Çankaya University until 2019. He is currently with the Department of Civil Engineering at Kadir Has University. His research interests include geotechnical earthquake engineering, soil-structure interaction, seismology, and deep learning applications in earthquake engineering.